# Table-top flash X-ray diagnostics of dodecane sprays

E. Robert*, S. Dozias, R. Viladrosa, C. Cachoncinlle and J.M. Pouvesle
GREMI, CNRS-Polytech'Orléans, 14 rue d'Issoudun, BP 6744,
45067 Orléans Cedex 2, FRANCE

**Abstract**

Time resolved radiography of pure dodecane and cerium doped dodecane sprays expanding through multi-hole production diesel injectors are reported for the first time using a table top flash X-ray source. The radiograph analysis indicates that strong mixing between liquid and ambient gas occurs in the very near nozzle region. The spray is described as two different density components having different penetration velocities. The cone angle, the penetration velocities and the liquid fraction value inferred from the radiographies are in relative good agreement with the recently published results involving very close injector and injection configurations and the reference X-ray diagnostics based on synchrotron radiation. This indicates that the mean energy analysis, required with the use of non monochromatic X-ray sources, appears as a reliable approach. Preliminary measurements of multi hole injection characteristics in a chamber inflated up to 30 bars of nitrogen are also documented. Considering the potential improvements likely to be implemented in future experiments, the table top flash X-ray radiography of diesel sprays may offer some promising alternative to the synchrotron studies.

## Introduction

The development and optimization of diesel engines faces many critical issues related to the search for the most efficient combustion conditions and the limitation of soot, $CO_2$, $NO_x$, and unburned hydrocarbons by-product emissions. Apart from the recent studies dedicated to the development of new biodiesel fuels, conventional diesel engines have been operated with higher and higher rail pressures to enhance the liquid spray evaporation. This progressive change in the engine working conditions has required both experimental and modeling efforts for the design and characterization of new injection strategies (injector design, injection duration or frequency), and combustion chamber. Significant progress have been achieved, essentially through high speed shadowgraphy or laser based diagnostic techniques such as LIF, LDA, PIV, etc., developed for the spray characterization in connection with modeling works. Unfortunately, the visible or UV light scattering in the dense near nozzle region consists in an intrinsic limitation preventing to obtain valuable experimental data in this specific zone. Besides neutron radiography [1], the unique non intrusive experimental technique reported up today to get a comprehensive description of the near nozzle spray behaviour is based on the soft X-ray absorption, such diagnostics being essentially developed at Argonne National Laboratory using synchrotron X-ray at the Advanced Photon Source [2-6] and the Cornell High Energy Synchrotron Source (CHESS) [7,8]. Some authors also report on the X-ray diagnostics of dense jets using laboratory sources with the whish to develop table-top user-friendly alternatives to the reference but access restricted experimental campaign using large synchrotron rings. Baev et al. [9] developed a portable pulsed, 20 ns exposure, X-ray source for the radiography of 250 µm in diameter jets. In that work, the use of a high voltage X-ray tube voltage of 100 kV requires a 1:1 doping with ethyl iodide of the fluid to achieved significant contrast with the high energy X-ray photons. Birk et al. [10] also developed flash X-ray radiography for the liquid core structure characterization of methyl iodide, 1 mm in diameter sprays expanding in high temperature and high pressure conditions. Char et al. [11] used very high voltage continuous X-ray source, powered with voltage of 160 and 320 kV, for the diagnostics of 2 mm in diameter water and pantopaque, a liquid including iodine. X-ray tomography [12] was recently used in comparison with optical laser techniques and high speed photography for the spray angle and liquid density distribution determination for 1 mm in diameter Shell fluid with no indication of any doping agent adjunction for the first time. Finally, a very recent paper [13] reports the first use of polycapillary optics in combination with a continuous X-ray micro focus x-ray source for the diagnostics of a 150 µm in diameter gasoline spray doped with a cerium based admixture. In all these works, the potentialities of X-ray diagnostics for the spray angle and liquid fraction measurements in the dense zone near nozzle orifice region in comparison with the optical visible techniques is emphasized and strengthen the effort for the development of such diagnostics considering the unique possibilities to get a comprehensive experimental analysis of the sprays likely to favour the development of physically sound modelling works. Compact flash X-ray sources have been developed in GREMI for years [14] in a large variety of applications, including soft X-ray diagnostics of dense gaseous [15, 16] and supercritical [17] jets. The development of compact X-ray pulsed sources, 20 ns exposure time, emitting strong doses on the 5 to 10 keV energy range, al-

* Corresponding author: eric.robert@univ-orleans.fr

low the radiography and X-ray induced fluorescence imaging of argon jets in ambient air and the first application of X-ray radiography for the diagnostics of pure, non doped, nitrogen cryogenic jets, 2 mm in diameter, evacuated in a high pressure chamber inflated up to 50 bars. Following our previous experiments on the development of flash X-ray diagnostics, this contribution deals with the time resolved diagnostics of dodecane injection through micrometric nozzles in a high pressure chamber, using a table top lab developed flash soft X-ray source. While providing less accurate data than highly monochromatic and space resolved synchrotron studies, time resolved, on nanosecond time scale, flash X-ray radiography allow for the determination of the near nozzle spray density together with the spray angle and propagation velocity in a large range of operating conditions including different injectors, chamber pressure, rail pressure, and fuel composition. For the first time to the best of our knowledge, the radiography of pure, non cerium doped, diesel like spray is documented and compared with a more fully detailed analysis of cerium doped sprays produced through two production type multi hole 150 µm and 110 µm in diameter injectors. It can be pointed out that such an approach dealing with multi hole production type injectors, and not single hole nozzle specially matched for experimental studies, has been very recently experienced at the APS facility [18-20], showing the influence of a more realistic configuration on the spray characteristics.

The next section presents the experimental setup including a brief description of the flash X-ray source designed for spray diagnostics. The calculation of the X-ray energy range of interest, the flash X-ray focus characteristics, the evaluation of the mean X-ray spectrum energy, and the spatial resolution and density measurement accuracy are documented in the third section devoted to the X-ray setup characterization. The next section then deals with the dodecane, both pure and cerium doped, spray diagnostics and conclusions are drawn in the last section of this manuscript.

**Experimental setup**

Fig. 1 presents the experimental setup used for spray diagnostics. It articulates around four main subassemblies: a flash X-ray source, a high pressure chamber, an X-ray CCD camera and a pilot for the triggering and synchronization of the X-ray source shots and the needle injector control.

The flash X-ray source relies on the production of nanosecond duration electric discharge across two electrodes inserted in a reactor maintained under vacuum, designed as the X-ray diode. The electron bombardment of the anode produces the largest portion of the X-ray flux in the characteristic lines of the used metal, while the Bremsstrahlung radiation resulting from the charged particle thermalization accounts for a few per cent of the whole X-ray spectra [21]. The flash X-ray source emits X-ray pulses having a typical duration of 20 ns. Taking into account the usual spray velocities, no motion blur is possible during radiography and the temporal resolution of the diagnostic can be as low as 20 ns. The diagnostics of diesel sprays requires the averaging of injection events over a few thousands X-ray shots to get a sufficient signal to noise ratio from radiographs performed on micron sized sprays, exhibiting typical absorptions of a few percent. The radiography of small size sprays performed with the use of a fully divergent X-ray beam, and not a parallel beam as in synchrotron based experiments, implies that the X-ray focus has to be set at a large distance from the jet location, typically at 100 cm, to simulate a point like focus and thus achieve a sufficient spatial resolution diagnostics. This latter constraint unfortunately induces a strong decrease of the X-ray flux at the jet position both because of the source divergence and the X-ray absorption in ambient air from the X-ray focus to the chamber entrance window. The best compromise was found with a distance from the X-ray diode output window to the spray axis of 125 cm. The X-ray dose measured at the X-ray diode output window are of a few hundreds of mR per shot. This corresponds to a typical X-ray flux emitted in the full space solid angle of $10^{11}$ X-ray photons per shot. At 1 m from the X-ray diode, the X-ray flux is lowered, following the inverse square function of the distance for a fully divergent source of radiation, down to a few $10^7$ photons/shot which corresponds to about 10 X-ray photons per shot per CCD (13 µm*13µm) pixel when including the air absorption for 8 keV photons over 1 m. This flux is even more reduced when the spray chamber is pressurized with nitrogen. Such consideration implies that the spray radiographies are obtained with averaging the signal over one thousand to a few thousands of injections and X-ray pulse events, i.e. with the accumulation of a few tens of thousands of X-ray photons per CCD pixel. This value is almost of the same order of magnitude as that estimated which could be estimated in the experiment reported with synchrotron source [2-5]. In this latter case, dealing with the APS facility, the very intense X-ray beam, about $10^{17}$ photons/s, is monochromatized ($10^{-4}$ bandwidth) and focused (0.5 x 0.3 $mm^2$ ) before being limited by vertical and horizontal slits (typically 250 µm x 50 µm in size). This corresponds to about $10^{11}$ monochromatic photons delivered at the spray position par second. With the point like avalanche photodiode detection setup used in most of spray characterization, the signals are obtained with an averaging over a few tens of about 3 µs duration exposures, the diameter of the photodiode probably being of about 20 µm when considering the measurement grids reported in some publications [5, 20]. All these considerations leads to the use of about 7000 X-ray photons per exposure that is the use of a few tens of thousands X-ray photons for each measurement in the mapping grid. These estimation are suggested to provide some comparison elements between the synchrotron and conventional soft X-ray diagnostics. It must nevertheless be pointed out that while the photon fluxes are

comparable, the extended focus and low monochromaticity of X-ray tubes still being some limiting factors. The development of more powerful flash X-ray source or their association with efficient X-ray optics would of course be of great interest for the improvement of their use in spray diagnostics as it may allow both for X-ray beam shaping and monochromatization.

Three common anode elements -iron, copper and tungsten-, can be used to produce X-ray photons in the energy window of interest for spray diagnostics. The higher X-ray fluxes are obtained with tungsten anodes but the X-ray spectrum is composed of several characteristic L lines which is not a very favourable situation for spray density calculation, ideally achievable with a monochromatic radiation. Iron electrodes exhibit the lower energy photons in the K lines around 6.4 keV but, in this case, the X-ray flux is much lower and the sputtering of the anode during electron bombardment is to high, impeding to operate this material in repetitive experiments over few thousands of shots. The best compromise between the X-ray flux, the long term flash X-ray operation and the contrast between the jet and the chamber absorption was found with copper based anodes. While pure copper anodes suffer from a dramatic sputtering over a few hundreds of shots, brass anodes were successfully experienced in this work. In this latter case, the use of cone shaped anode, which tip position relatively to the ring cathode plane can be easily adjusted during experiments, was measured to result in a good stability of the X-ray flux during a few tens of thousands of shots. For all the measurements presented in this work, the voltage pulse across the electrodes was of 30 kV.

The spray chamber is a 1 $dm^3$ stainless steel vessel equipped with a port for the injector insertion, one entrance and one output ports along the X-ray propagation path, one port for the pressurization up to 30 bars and a last one to evacuate the chamber down to atmospheric pressure. The bottom flange of the chamber is equipped with an evacuation pipe and an inner trap to prevent from fuel accumulation and sputtering during injections. Different Bosch production injectors can be successively set in the chamber. The injector axis is located 75 mm away from both the front and back flanges of the chamber, along the X-ray penetration path. The injector nozzle is equipped with a spray selection shield which allows that only the vertical spray expands in the chamber while the fuel ejected through the other orifices is trapped in the shield volume and finally flows down to the bottom flange through a plastic pipe. This shield reduces the fuel vaporization in the chamber. The fluid used for injection is dodecane 44020, $C_{12}H_{26}$ from Sigma-Aldrich. The injector pilot monitors rail pressures up to 1200 bars, controls the injection duration, the injection repetition rate, triggers the flash X-ray source and set delay between the X-ray shot and the injector needle activation. The jitter between the X-ray shot and the injection signal was measured to be around 10 ns which is negligible regarding the dynamics range for diesel spray characterization.

The detector used for X-ray radiography consists in an Andor DY432-FI-DD X-ray CCD camera equipped with a low energy beryllium entrance window. The camera is fixed on the high pressure chamber. Circular windows, 8 mm in diameter or rectangular slits (5 mm wide, 24 mm high) equipped with 125 µm thick Kapton® films, with high X-ray transmission, have been used as entrance and exit windows along the X-ray propagation path from the X-ray source to the CCD camera.

## Flash X-ray characterization

Following our previous developments, a flash X-ray source was specially designed for the diagnostics of diesel spray in a high pressure chamber. The main features of such diesel sprays in connection with the requirements for an X-ray based diagnostics have been considered, for the best matching of the X-ray flash generator for the spray characterization. The most critical specificities consist in the low Z element -carbon and hydrogen- composition, the high velocity -up to a few hundreds of $m.s^{-1}$-, and the micro size of the spray evacuating in a high pressure -a few tens of bars- atmosphere. There exists a real interest for the measurement of the spray topography, depth of penetration, angular aperture, radial and longitudinal expansion, velocity, and density in the near nozzle region, i.e. over the first tens of orifice diameters from the nozzle outlet.

### *X-ray energy range*

The typical orifice diameter of serial injectors ranges from about 100 µm to 250 µm. For practical and safety reasons and to try to obtain relevant comparisons between the new developed near nozzle diagnostics with the conventional laser based measurements obtained at larger distances from the nozzle outlet, most of the experiments are performed in chambers filled up to a few tens of bars such as nitrogen [5, 6, 18-20] or SF6 [2-4]. This allow for a first approach of engine-like high density ambiance [5, 6, 18-20]. The penetration path across the high pressure chamber generally consists in a few centimetre long channel, the chamber being closed with windows compatible with a few tens of bars working pressure. Fig. 2 presents the X-ray transmission along a penetration path including two 125 µm thick Kapton® windows, equipping the high pressure chamber, and a 15 cm thick layer of nitrogen in comparison with the penetration across the same windows, a 14.989 cm thick nitrogen layer and a 110 µm thick carbon layer having the pure dodecane density of 0.75 $g.cm^{-3}$. These calculations [22], corresponding to the diagnostics parameter documented later in the manuscript, are performed for chamber pressure of 1 and 10 bars and the ratio between the X-ray transmission through and out of the jet, termed as the

"contrast", up to 15 keV is also illustrated on top of Fig.2. It appears that the lower the X-ray energy is, the higher the contrast is but that the chamber transmission is below 1% for X-ray energies lower than respectively about 3.5 and 5.5 keV for 1 and 10 bars working pressure respectively. On the other hand, the ratio between the transmission through and out of the jet is lower than 1.01, i.e. the transmission contrast is lower than 1%, for X-ray energies higher than 12 keV. These characteristics indicate that the X-ray energy range likely to allow for pure diesel spray diagnostics is limited from about 6 to 12 keV. The full thin traces, plot the transmission and contrast obtained at one bar when the 110 µm thick layer is doped with 0.5% of cerium. The lower energy transmission limit is almost unchanged in comparison with the pure dodecane configuration while the contrast is very significantly enhanced near the cerium absorption edges around 6 keV but also up to 15 keV. In this work, the first experiments have been performed on pure dodecane sprays, and successive diagnostics were then obtained on cerium doped sprays as documented in all synchrotron based publications. The main goal was first to check for the influence of such heavy element (Z=58) adjunction in the propagation and density of the spray before collecting a more detailed data set with the use of this additive which results in a higher contrast for X-ray photons.

***Mean X-ray spectrum energy***

Following the approach from Curry et al. [23, 24], the average X-ray spectrum energy of the flash X-ray source used in this work was determined. This average energy measurement is required for the spray density calculation using a non monochromatic X-ray source. For this purpose, the X-ray transmission of 125 µm thick Kapton® ($C_{22}H_{10}O_2N_2$) scales with a 1.42 g.cm$^{-3}$ density and 90 µm thick film scales of polymethylpentene (TPX®) with a 0.83 g.cm$^{-3}$ density were performed. These experiments correspond to very close conditions to the spray characterization whose typical diameter is between 100 and 250 µm and which maximum density is that of pure dodecane, i.e. 0.75 g.cm$^{-3}$. The measurement of these test object transmission was realized over a 1000 X-ray shots in the same configuration as that used later for spray diagnostics. The distance between the X-ray focus and the film scale was set to 125 cm, the distance from the film to the X-ray CCD camera was set to 75 mm, and two additional 125 µm thick Kapton® layers were inserted, one in front of the object, and the other in front of the camera, to integrate the ambient air and the high pressure chamber window filtering. In these experimental conditions, the mean X-ray energy was determined to be of 8.3 keV, this value being consistent with the emission of the characteristic Kα copper line and the zinc Kα characteristic line over a much less intense Bremsstrahlung spectrum [21]. Complementary experiments were finally performed using 200 µm thick liquid test layer composed of dodecane or water. The 200 µm liquid film was realized in a specific holder including two 8 mm in diameter region, one of this region being filled with air at atmospheric pressure while the other is filled with either dodecane or water. This experiment confirms the 8.3 keV mean energy and allows checking the density value of the dodecane used during spray characterization. The measured X-ray transmission are of 0.93 and 0.82 respectively in very good agreement with the theoretical values for an 8.3 keV energy, of respectively 0.939 and 0.83 obtained from the cxro calculator [22].

***X-ray focus characteristics and X-ray diagnostics spatial resolution***

To determine the size of the X-ray focus, pinhole imaging experiments were performed using a 200 µm in diameter, 1 mm thick lead pinhole. The pinhole plane was set 10 cm from the X-ray flash while the X-ray CCD camera was set 40 cm away from the pinhole. Accumulation over 1000 shots was performed to be representative of the spray diagnostic conditions. The X-ray focus is about 500 µm in diameter and the X-ray focus moves from shot to shot around a ring having a mean diameter of 1 mm. The X-ray focus over a few hundreds of shot thus consists in a 500 µm thick ring which internal diameter coincides with the intersection of the anode tip with the cathode plane. This relative position of the electrodes is continuously adjusted during the diagnostic experiments and empirically corresponds to the best separation between both electrodes which undergoes the strongest X-ray fluxes for a fixed voltage difference across the X-ray diode. A windowless PIN photodiode allows for the monitoring of the X-ray pulse intensity. It was experienced that smaller X-ray focus size can be achieved for smaller gaps between the X-ray diode electrodes but unfortunately induce X-ray flux lowering and more important shot to shot fluctuation leading to a very less reproducible average X-ray flux from one radiograph to another.

The resolution of the full X-ray radiography setup was first inferred from the analysis of the grey level profiles extracted from the radiograph of a test pattern graduated with 0.1 mm thick lead and air line pairs with a number of line pair per mm ranging from 1 (1 mm basic pattern) to 5 (100 µm basic pattern). Fig. 3 presents the grey level profiles obtained in the geometrical configuration of the spray radiography (X-ray focus to object and object to X-ray CCD distances of respectively 125 cm and 75 mm, averaging over 1000 shots) with a vertical CCD binning over 10 mm. Fig. 3 illustrates that significant contrasts are obtained for patterns as small as 100 µm. The calculation of the modulation transfer function involving the ratio of the peak to valley grey level amplitudes to the maximum grey level value amplitude, for the different spatial frequencies, associated with the number of line pairs per mm, together with the calculation of the signal to noise ratio, result, with this classical

approach, in a resolution of 120 µm. This value appears appropriated for the spray diagnostics proposed in this work considering that no detailed analysis of the radial spray properties could be inferred from our measurements at the present level of development of the flash X-ray diagnostics. Finally, radiographies of four nylon ($C_{12}H_{22}O_2N_2$ with a density of 1.15 g.cm$^{-3}$) fishing threads with diameters of 60, 100, 140 and 180 µm were performed to quantify the density calculation accuracy on micrometric cylindrical object having a density close to that of dodecane. Such measurements were performed four times with an averaging over 1000 X-ray shots to obtain an estimation of the density value standard deviation inferred from radiographs. The density was calculated with accounting for an average X-ray energy of 8.3 keV as already discussed. The density deviates from the theoretical value for nylon from 4 ± 2 %, 12 ± 11 %, 25 ± 13 %, and 32 ± 13 % for fishing thread diameter of 180, 140, 100 and 60 µm respectively. This measurement indicates that for objects having a dimension above the resolution limit of the X-ray set up, the deviation in the density calculation from radiograph is lower than about 20 % which is of course much less accurate than in synchrotron studies but nevertheless represents a rather appreciable estimation of this parameter using a table top facility.

## Spray diagnostics

### *Pure dodecane sprays*

Fig. 4 presents the radiographs, obtained over 3000 X-ray shots, of pure dodecane injection through a kf0, 6 hole injector having orifice diameters of 150 µm. The rail pressure is of 800 bars and the injection duration is of 500 µs. If the time origin is arbitrarily set to zero for the left picture, the respective delays of the other radiographs with respect to this time origin are of 10, 15, 25, 40 and 65 µs from left to right. To the best of our knowledge, this result is the first X-ray measurement of pure dodecane spray where no additive was added to enhance the contrast while being obtained in a multi hole production type injector. From this limited quality radiograph we deduce three essential features which will then be confirmed and described in more details in the next section.

First the propagation of the spray from the nozzle outlet occurs with a velocity of about 40 m.s$^{-1}$ considering the three first delays, and then speeds up to about 150 m.s$^{-1}$ when considering the three longer delays documented in Fig. 4. This a priori non evident behaviour in the near nozzle region of the spray, as on the contrary to our observations one would expect a deceleration during the injection through the interaction of the spray with the ambient gas pressure, was recently reported [6, 19] and attributed to the observation of the first instants of the spray penetration in the nozzle outlet vicinity which corresponds to a stage when the injector needle is not yet fully opened. No evidence for a pronounced higher density spray region at the leading edge position is observed in our experimental conditions. This dense leading edge structure was shown to be very obvious [2-4] for spray expansion in $SF_6$ ambience while being somewhat less diffuse [6] in nitrogen chamber, and quite absent for multi hole nitrogen chamber conditions [18-20].

The second observation concerns the geometrical shape of the spray averaged over 3000 X-ray shots. It is observed that the spray propagation occurs in a very stable fashion from one injection event to another as no indication for a deviation over a significant number of spray propagation paths from the averaged radiograph signal documented in Fig. 4 is measured on the radiograph. The full angle of aperture, inferred from the measurement of the ratio of the radial extension to the downstream propagation length at the different instants during the spray penetration, has a constant value during the first 100 µs of the injection of about 5° with no significant evidence for the presence of dodecane out of this cone. Such small cone angle value in comparison with the much larger values reported with visible or UV light diagnostics was previously reported in synchrotron works: less than 5° cone angle [2] in $SF_6$ filled chamber, small cone angle value which evolves during the spray expansion in relation with mass accumulation in the leading edge of the spray [3], evolution from 2.5° to 7° during injection event in $N_2$ ambiance [18]. At the difference of the results reported in [20] of a larger cone angle of about 10°, associated with a multi hole and not a test single hole nozzle, our results show no correlation with the multi hole characteristics of the nozzle on the cone angle enlargement as will be confirmed later in this manuscript. No evolution of the spray cone angle during the first 100 µs of fuel injection was also evidenced in our experimental conditions.

Finally, the maximum density inferred from the ratio grey level value measured in and out of the jet and accounting for an average X-ray energy of 8.3 keV and the dodecane X-ray absorption cross section for this X-ray energy, is of about 0.45 g.cm$^{-3}$. The spatial resolution limitation of our diagnostics, involves that no radial analysis of the spray density can be inferred from the radiograph, the density is then estimated considering an averaged cylindrical spray diameter. The spray thickness is zero on the spray border while being that of the nozzle orifice diameter at the nozzle outlet. The density value of the dodecane spray density is very low in comparison with that of an ideally pure liquid core, as accounted for in the modelling studies at least over the first diameters downstream the nozzle injector. Our measurements have no sufficient spatial resolution to conclude that such a pure liquid structure exist or not in the very close vicinity of the nozzle outlet, i.e. over the first 0.3 mm, but the

spray density averaged over the first 1 millimetre long propagation zone traduces a strong mixing of the dodecane with the ambient gas. The fit of the measured X-ray transmission with the calculation for 8.3 keV incident energy photons, leads to the conclusion that the pure liquid fraction represents less than 60% over the first 300 µm. This very significant mixing of the liquid phase with the gas in the near nozzle region was also previously reported [2, 3] and confirmed for multi hole nozzles [18-20].

Once again, all these observations are deduced from relatively poor contrast radiograph but will be largely confirmed in the next section dealing with cerium doped sprays. The main interest for this report lying in the first measurement of diesel like spray through production type injectors in non high Z element doped sprays, which was never published to the best of our knowledge.

***Cerium doped sprays***

A blend of dodecane with cerium was mixed with pure dodecane in a 0.5 % volume fraction corresponding to a 4 % by weight Ce concentration. This additive is used in engine technology for the regeneration of diesel filters issues but also has a strong impact on the X-ray diagnostics due to the strong photon absorption of cerium around 5.7 keV and above. For an 8.3 keV average X-ray energy, the transmission of a pure liquid dodecane cylinder of 110 µm in diameter, as will be documented below, is of 0.968 while the combination of a 109.45 µm thick dodecane with a 0.55 µm thick (0.5 % volume fraction) cerium (density 6.77 $g.cm^{-3}$) layers results in a whole transmission of 0.849. These data illustrate the very significant influence of a small cerium addition on the X-ray transmission and the resulting improvement on the radiography contrast as previously depicted in figure 2.

Fig. 5 presents the dynamics of the Ce doped dodecane spray through the kf0, 6 hole injector having outlet diameters of 150 µm already characterized with pure dodecane in Fig. 4. Each radiograph is averaged over 1000 X-ray shots, three times less than for pure dodecane, and the delay with respect to the start of injection on the left picture is incremented by 10 µs steps from the left to the right in Fig. 5. While the diagnostic is performed for one third of injection and X-ray shot events, the radiograph quality is much better than for pure dodecane. The analysis of the radiograph confirms the essential features of spray expansion at atmospheric pressure. The velocity appears to increase after the fourth instant if one applies a linear fit between the spray leading edge limits measured on each radiograph. The cone expansion occurs with a very comparable aperture angle and the lowest transmission measured on the radiograph in the near nozzle region reveals a liquid fraction lower than 60 %.

Fig. 6 presents the dynamics of Ce mixed sprays through another, ks1.5, 6 hole injector having a different cavity geometry and outlet injector diameters of 110 µm. Each radiograph is averaged over 1000 X-ray shots and the time increment between each radiograph is again of 10 µs corresponding to instants ranging form the start of injection (left picture) to 100 µs for the righter radiograph. A more detailed analysis of the radiograph was performed from this latter injection dynamic recording. Fig. 7 presents the grey level longitudinal profiles, extracted from the 20, 40, 60, 80 and 90 µs snapshots with a radial binning over a constant width corresponding to the full width of the spray at the outlet position. With this analysis, an increasing portion of the spray is not considered due to the spray radial expansion as the distance from nozzle outlet increases. For each of these 5 instants, Fig. 7 presents first a flat profile obtained out of the spray axis to evaluate the flat field illumination of the CCD camera during flash X-ray exposure and to illustrate the signal to noise ratio level. For each five instants, Fig. 7 also presents the spray longitudinal profiles centred on the spray axis. The grey level vertical scale was normalized for each instant to the mean out of axis profile amplitude so that the vertical scale indicates the transmission of the spray as a function of the downstream position from the nozzle outlet. The spray longitudinal profiles exhibit up to three different sections illustrated by the lines added on Fig. 7 for the clarity of the discussion. The lower transmission is measured at the nozzle outlet and then gradually increases up to a constant value which is preserved up to the leading edge of the spray indicated by the position for which the transmission starts to increase up to the unity, that it where the jet vanishes and the X-ray transmission is the same on the jet axis and out of axis. For instance, for the 80µs instant, the transmission evolves from the origin up to the 3 mm position, then stabilizes to a rather constant value from the 3 to the 8.5 mm positions and the jet leading edge is measured around the 11 mm position. These positions evolve during the spray expansion. The positions of the "dense component" spray portion, at the nozzle outlet, and of the spray leading edge are plotted in Fig. 8 as a function time during the spray expansion. A quite continuous evolution of both the "dense component" and the "leading edge" penetration in the chamber is measured up to 100 µs. It is worthwhile observing that the dense component and spray leading edge mean velocities over the first 90 µs from the start of injection are respectively of 44 $m.s^{-1}$ and 128 $m.s^{-1}$ in very good agreement with those for pure dodecane sprays where 40 $m.s^{-1}$ and 150 $m.s^{-1}$ values were estimated from Fig. 4. This is an additional indication that the cerium adjunction and the orifice diameter, from 110 µm to 150 µm, have no very crucial influence on the spray expansion.

The analysis in the radial direction of the grey level profiles longitudinally averaged from the nozzle outlet up to 15 mm downstream for three different instants during the spray expansion is proposed in Fig. 9. The averaging along the longitudinal axis of the spray was of 0.4 mm for the three first positions and was then processed over a 1.1 mm height for the larger downstream positions. The radial full width at half maximum was extracted from each grey level profiles and plotted as a function of the downstream position. Fig. 9 reveals that the cone jet an-

gular aperture is constant from the first instants to the later times during the spray propagation as each set of data could be fitted by a same slope straight line. While the jet exhibits a two component structure, revealed by Fig. 7 profiles, having two different velocities, it appears that the angular dispersion is constant and that the dense and spray leading edge portion expand in the same way in the radial direction. The full aperture angle inferred from Fig. 9 is of 5.7°, once again in very good agreement with the value estimated for the non cerium doped spray.
The calculation of the projected mass as the product of the spray density, inferred from figure 7, times the spray thickness plotted in figure 9, 80 µs after the start of injection, is proposed in figure 10 in comparison with data extracted from reference [19] for a 5 hole production nozzle, 130 µm in diameter, a rail pressure of 800 bars, injection duration of 1 ms and injected in a nitrogen chamber at one bar. These latter conditions [19] being very close to our experimental parameter, i.e. 6 holes, 110 µm, rail pressure 800 bar , injection duration 500 µs, one bar nitrogen chamber. The fit proposed in Fig. 10 for the sampled data from [19] is worse than that achieved through the full data set. The main conclusion from figure 10, is that while exhibiting a larger signal to noise ratio, our measurement presents a rather good agreement with that obtained with synchrotron facility. The fluid density was not indicated in [19] but was probably very close to 0.8 $g.cm^{-3}$. Correspondingly with the measurement proposed in Fig. 10, the liquid fraction is of 65% at the nozzle exit and rapidly falls down to around 10%, 3 mm downstream when accounting for the cone expansion and supposing a constant radial density over the mean spray diameter imaged by X-ray photons.

***Diagnostics at higher pressure chamber***

Preliminary experiments have been performed when inflating the chamber with nitrogen up to 30 bars. Fig. 11 presents two radiographs obtained with the ks1.5, 6 hole injector having outlet orifices of 110 µm in diameter operated with a rail pressure of 800 bars with the cerium doped dodecane mixture. In this experiment, the chamber is inflated at 25 bars of nitrogen which corresponds to a reduction of the 8.3 keV X-ray incident flux on the CCD camera by a factor of 14 in comparison with that at one bar [22]. The two radiographies are performed over 1000 injection events and correspond to delay of 20 and 70 µs after the start of injection. While the signal to noise ratio is much smaller than for atmospheric pressure operation, the spray propagation is observed. The spray leading edge, indicated in Fig. 11 by the vertical marks, is unambiguously measured from the grey level profile analysis.

The table I summarizes the measured penetration of the spray leading edge for the two delays as a function of the chamber pressure for 1, 13 and 25 bars. As awaited, the spray penetration is reduced as the chamber pressure increases. The mean velocity between the 20 and 70 µs instants drops from 255 to 220 and 138 $m.s^{-1}$ as the chamber pressure is increased from 1 to 13 and 25 bars. On the other hand the spray cone angle appears rather independent of the chamber pressure in this first approach of high pressure injection study. While these results appear somewhat contradictory with those recently reported [5], the average over a larger number of X-ray shot should improve the radiograph quality and allow a more detailed analysis of the spray expansion for high chamber density.

**Conclusion**

A table top flash X-ray source emitting X-ray pulses of nanosecond duration was developed for the diagnostics of dodecane sprays expanding through micrometric orifice in a high pressure chamber. The consideration of the relative absorption of carbon based sprays about 100 µm thick with that of a centimetric nitrogen layer at pressure ranging from one to 30 bars imposes the development of an X-ray source radiating low X-ray energy photons below 10 keV. The requirements in term of spatial resolution to achieve a reliable description of the radial and longitudinal jet profile over a few tens nozzle orifice diameters along the spray propagation path from a divergent X-ray focus imposes a large distance, set at 125 cm in this work, between the X-ray focus and the spray axis. With such objectives, a flash X-ray source delivering high flux of X-ray photons from a brass anode was designed, optimized and shown to be capable of repetitive operation over a few thousands of X-ray shots. The spatial resolution of the full diagnostic assembly, including the flash X-ray source and an X-ray CCD camera was analyzed with the use of calibrated patterns having basic features as small as 100 µm. The accuracy of the density measurement from the grey level analysis measured on the radiographies was inferred from experiments performed on micron size fishing threads having density comparable to that expected for fuel sprays. Various experiments were performed to measure the average equivalent X-ray energy of the flash X-ray source which was of 8.3 keV. This procedure is mandatory to select the X-ray absorption cross section required to determine the spray density from the measured X-ray transmission value. Successful diagnostic of dodecane sprays was then processed and documented in this manuscript with the use of multi hole production injectors. The first experimental radiography of pure, non doped, dodecane spray expansion was performed and allow the characterization of the spray cone angle, the measurement of the velocity and its evolution from the start of injection and during the jet expansion. It also evidences a strong mixing of the liquid fraction of the spray with ambient air in the very near nozzle region. Cerium additive was then added to the dodecane and a more detailed analysis of

the sprays was proposed for 150 and 110 µm orifice diameter nozzles. A very close behavior was measured when using the same injector, the same rail pressure and the same injection duration but for pure and cerium doped sprays. This observation justify the possibility to get a relevant description of fuel spray properties while adding a few per cent of cerium which undergoes a very significant x-ray contrast improvement and radiograph quality. The analysis of longitudinal grey level profiles then show evidence for the existence of a dense component in the near nozzle region and of a constant density spray leading edge part. These two spray components present different velocities but expand with the same cone angle as inferred from the radial profile measurements at different instants during the spray propagation. The strong mixing of the liquid fraction of the spray with ambient atmosphere was confirmed for cerium doped dodecane sprays. Finally the first experiments dealing with the influence of the chamber pressure were performed with nitrogen filling up to 30 bars. The decreases of the jet penetration depth and penetration velocity in the chamber were measured when the chamber pressure increases while no corresponding critical modification of the spray cone angle was measured. The pure dodecane spray diagnostics was achieved with a 3000 injection event averaging, while cerium doped spray radiographies were recorded with a 1000 averaging from one to 30 bars.

At the state of its development, the table top flash X-ray diagnostics of fuel sprays was shown to be possible and to allow for a screening of injectors, chamber pressure, rail pressure, injection duration, spray composition influence on the geometrical properties such as cone angle, dense and leading edge components. It also offers the possibility for such a parametric study with the measurement of the spray components velocities and density with an accuracy ranging from about 5 to 20 % for orifice diameter ranging from 200 to 100 µm respectively. While being less accurate than synchrotron diagnostics which offers unique possibility in term of monochromaticity and spatial resolution, the cost and cost of operation of our diagnostics might be an interesting alternative for a first approach of spray characterization requiring a large parametric study. Finally, the flash X-ray diagnostic can offer, even if it was not yet exploited in this work, a temporal resolution as low as about 20 ns which may be of interest for the description of some peculiar aspects of the fuel spray expansion.

**Acknowledgments**

This work is supported by GIE PSA-Renault program “Emphase”. The authors would like to thank Gregory Blokkeel for cerium dopant supply and scientific discussions.

**References**

[1] N. Takenaka, T. Kadowaki, Y. Kawabata, I.C. Lim, C.M. Sim, “Visualization of cavitation phenomena in a Diesel engine fuel injection nozzle by neutron radiography”, Nuclear Instruments and Methods in Physics Research A, vol.542, pp; 129-133, 2005.

[2] C. F. Powell, Y. Yue, R. Poola, and J. Wang, “Time-resolved measurements of supersonic fuel sprays using synchrotron X-rays”, J. Synchrotron Rad., vol. 7, pp. 356-360, 2000.

[3] Y Y. Yue, C. F. Powell, R. Poola, and J. Wang, J. K. Schaller, “Quantitative measurements of diesel fuel spray characteristics in the near-nozzle region using x-ray absorption”, Atomization and sprays, vol. 11, pp. 471-490, 2001.

[4] J. Wang, “X-ray vision of fuel sprays”, ”, J. Synchrotron Rad., vol. 12, pp. 197-207, 2005.

[5] A. L. Kastengren, C. F. Powell, Y. Wang, K. -S. Im, and J. Wang, “X-ray radiography measurements of diesel spray structure at engine-like ambient density” ILASS Americas, 21st annual conference on liquid atomization and spray systems, Orlando, FL, May 2008.

[6] A. L. Kastengren, C. F. Powell, K. -S. Im, Y. -J. Wang, and J. Wang, “Measurement of biodiesel blend and conventional diesel spray structure using X-ray radiography”, Journal of Engineering for Gas Turbines and Power, vol. 131, 062802-1-062802-7, 2009.

[7] W. Cai, C.F. Powell, Y. Yue, S. Narayanan, and J. Wang, “Quantitative analysis of highly transient fuel sprays by time-resolved x-radiography”, Appl. Phys. Letters, vol.83, pp.1671-1673, 2003.

[8] A.G. MacPhee, M.W. Tate, C.F. Powell, Y. Yue, M.J. Renzi, A. Ercan, S. Narayanan, E. Fontes, J. Walther, J. Schaller, S.M. Gruner, and J. Wang, Science 295, pp.1261-1263, 2002.

[9] V.K. Baev, A.N. Bazhaikin, E.I. Bichenkov, A.A. Buzukov, R.L. Rabinovich, and B.P. Timoshenko, “X-ray pulse method for investigation of the internal structure of a fuel jet”, J. Appl. Mech. Tech. Phys., vol. 21, pp. 97-103, 1980.

[10] A. Birk, M. McQuaid, and M. Gross, “Liquid core structure of evaporating sprays at high pressures-flash X-ray studies, ICLASS-94, 6th International Conference on Liquid Atomization and Spray Systems, Rouen, France, publication n° IV-11, pp. 459-66, 1994.

[11] J.M. Char, K.K. Kuo, and K.C. Hsieh, “Observations of breakup processes of liquid jets using real-time x-ray radiography”, Nasa technical report, document ID 19890001789, accession number 89N11160, pp.125-133, 1988.

[12] B. Balewski, B. Heine, and C. Tropea, "Experimental investigation of the correlation between nozzle flow and spray using LDV, PDA, High-speed photography and X-ray radiography", 8th International Conference on Liquid Atomization and Spray Systems, paper ID ILASS08-015, Como Lake, Italy, 2008.
[13] L. Allocca, L. Marchitto, S. Alfuso, D. Hampai, G. Cappuccio, and S.B. Dabagov, "Polycapillary X-ray imaging of a gasoline spray", 20th International Congress on X-ray Optics and Microanalysis, Karlsruhe, Germany, 2009.
[14] J.M. Pouvesle, C. Cachoncinlle, R. Viladrosa, E. Robert and A. Khacef, ''Compact flash X-ray sources and their applications'', Nucl. Instrum. Meth. Phys. B, vol. 113, 134, 1996.
[15] J. Geiswiller, E. Robert, L. Huré, C. Cachoncinlle, R. Viladrosa, and J.M. Pouvesle, "Flash X-ray radiography of argon jets in ambient air", Meas. Sci. Technol., vol. 9, pp.1537-1542, 1998.
[16] E. Robert, L. Huré, C. Cachoncinlle, R. Viladrosa, and J.M. Pouvesle, "Simultaneous X-ray induced fluorescence imaging and radiography of argon jets in ambient air", Meas. Sci. Technol., vol. 10, pp.789-795, 1999.
[17] B. Metay, E. Robert, R. Viladrosa, C. Cachoncinlle, J.M. Pouvesle, W. Mayer, and G. Schneider, "X-ray diagnostics of the near injector zone of cryogenic nitrogen jets at supercritical pressurees", proceedings of SPIE, vol. 4948, pp. 568-573, 2003.
[18] P. Leick, T. Riedel, G. Bittlinger, C.F. Powell, A.L. Kastengren, J. Wang, "X-ray measurements of the mass distribution in the dense primary break-up region of the spray from a standard multi-hole common-rail diesel injection system", proceedings of the 21st ILASS, annual conference on liquid atomization and spray systems, Europe meeting, 2007.
[19] P. Leick, A.L. Kastengren, Z. Liu, J. Wang, and C.F. Powell, "X-ray measurements of mass distribution in the near-nozzle region of sprays from standard multi-hole common-rail diesel injection systems", ICLASS 2009, 11th triennial International Annual Conference on Liquid Atomization and Spray Systems, Vail, Colorado, 2009.
[20] A.I. Ramirez, S. Som, S.K. Aggarwal, A.L. Kastengren, E.M. El-Hannouny, D.E. Longman, and C.F. Powell, "Quantitative X-ray measurements of high-pressure fuel sprays from a production heavy duty diesel injector", Exp. Fluids, vol. 47, pp.19-134, DOI 10.1007/s00348-009-0643-4, 2009.
[21] E. Romero, C. Cachoncinlle, E. Robert, R. Viladrosa, S. Dozias, G. Coudrat, and J.M. Pouvesle, "Characterization and optimization of a flash X-ray source for diagnostic of dense sprays", UVX2008, EDP Sciences, DOI:10.1051/uvx/2009029, pp. 177-181, 2009.
[22] http://henke.lbl.gov/optical_constants/. B.L. Henke, E.M. Gullikson, and J.C. Davis., "X-ray interactions: photoabsorption, scattering, transmission, and reflection at E=50-30000 eV, Z=1-92", Atomic Data and Nuclear Data Tables, vol. 54 (no.2), pp. 181-342, July 1993.
[23] J. J. Curry, M. Sakai, and J. E. Lawler, "Measurement of the Hg distribution in a high-pressure arc lamp by x-ray absorption", J. Appl. Phys., vol.84, pp. 3066-3072, 1998.
[24] J. J. Curry, "Quantitative x-ray absorption imaging with a broadband source: application to high-intensity discharge lamps", J.Phys.D:Appl.Phys., vol. 41, 144020, 2008.

**Table 1.** Spray leading edge penetration (mm)

| | Delay after start of injection | |
|---|---|---|
| Chamber pressure | 20 µs | 70 µs |
| 1 bar | 1.1 | 13.8 |
| 13 bars | 0.7 | 11.7 |
| 25 bars | 0.5 | 7.4 |

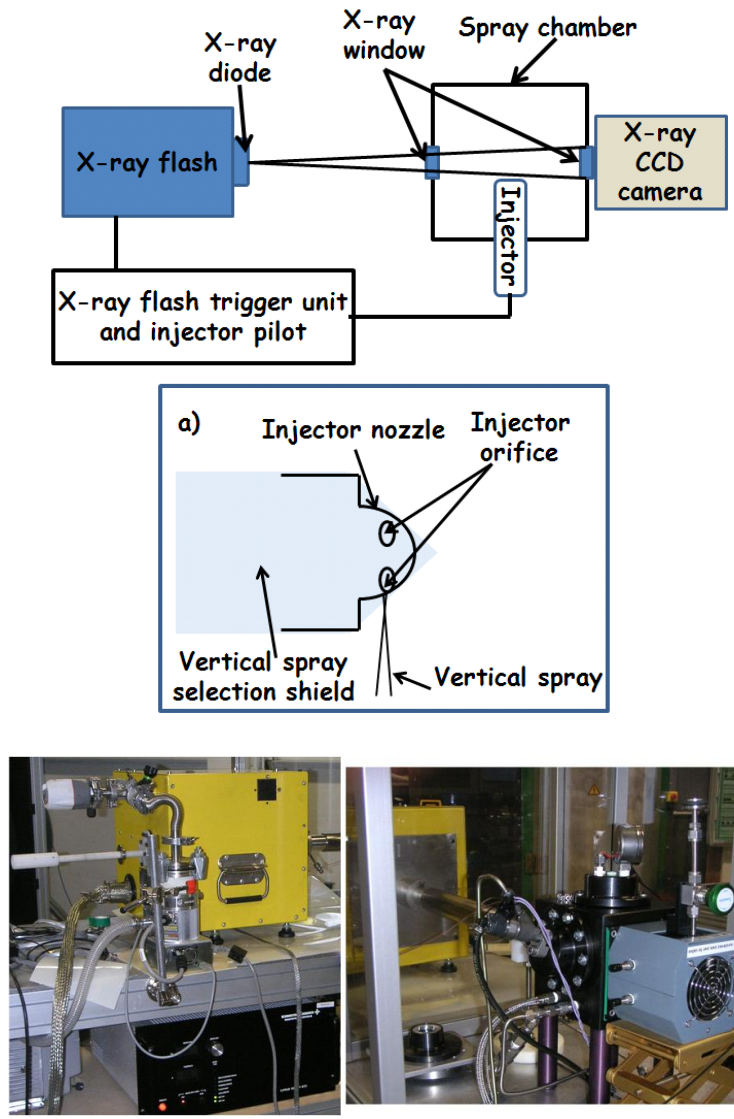




**Figure 1.** Experimental setup, inset a) illustrates the injector nozzle. Photo on the left shows the flash X-ray source, and photo on the right details the spray chamber (black) equipped with the X-ray camera

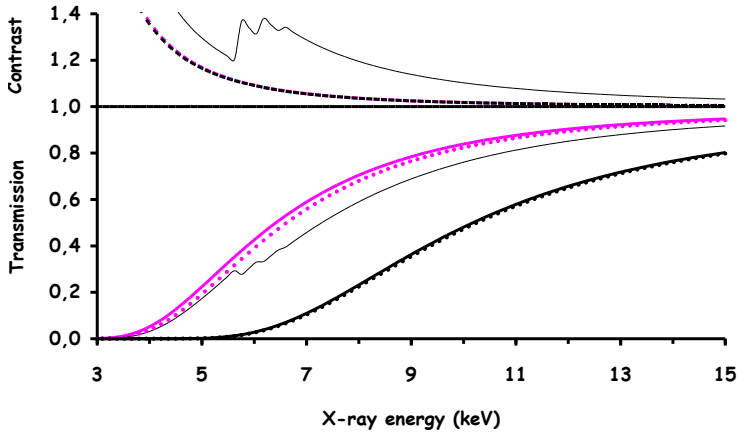


**Figure 2.** Light, respectively black dots represent on jet axis chamber transmission for 1 and 10 bars nitrogen filling, the jet is a 110 µm thick carbon layer 0.75 g.cm$^{-3}$ in density. Light, respectively black thick traces represent the off jet axis transmission for the same pressures. The thin black trace is on axis transmission of a 110 µm, 0.5% cerium doped spray for 1 bar pressure chamber. Top: light, respectively black dashed traces represent the contrast for 1 and 10 bars. Thin trace is the contrast for Ce doped jet at 1 bar

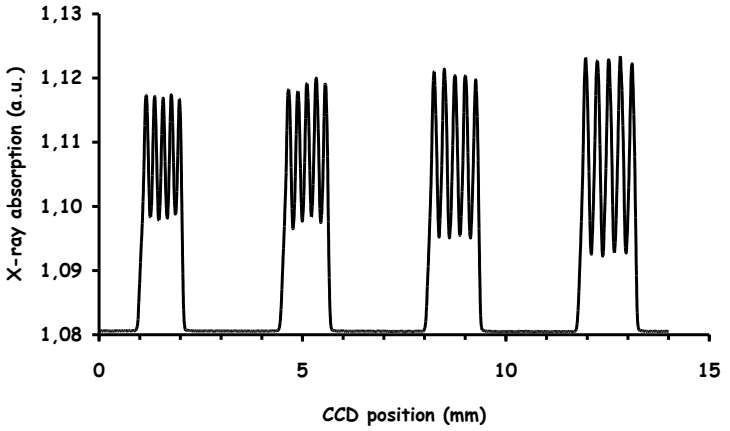


**Figure 3.** Grey level profiles from the radiograph of a calibrated line pair pattern. From left to right, the patterns consists in 5, 4.5, 4 and 3.6 line pairs per mm

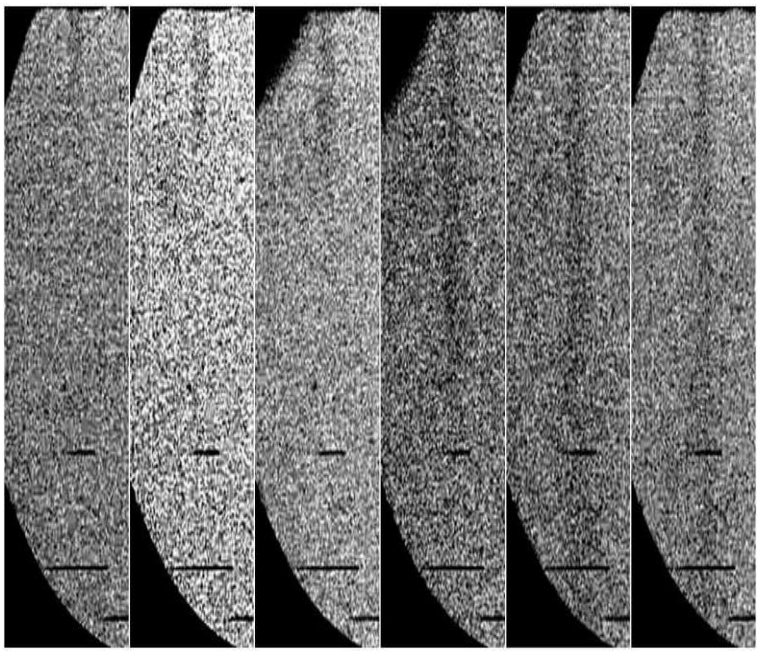

**Figure 4.** Pure dodecane spray radiographies. Rail pressure 800 bars, injection 500 µs, chamber pressure 1 bar, kf0, 6 hole production nozzle with orifice diameters of 150 µm on top center of pictures. Each radiograph is averaged over 3000 injection events, delays from left to right are 0, 10, 15, 25, 40 and 65 µs

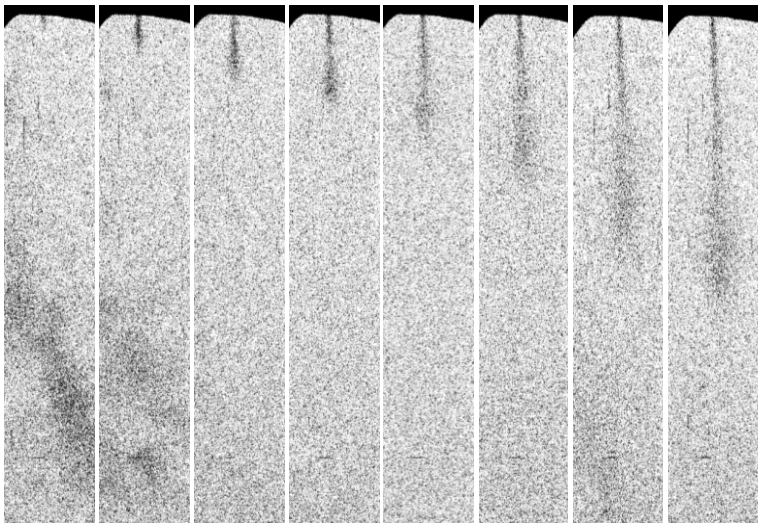

**Figure 5.** Expansion of dodecane/cerium spray through kf0, 6 hole 150 µm in diameter orifices, production nozzle. Rail pressure 800 bars, injection 500 µs, chamber pressure 1 bar. Each radiograph is averaged over 1000 injection events. The time increment is of 10 µs from start of injection on the left to the righter picture 70 µs later

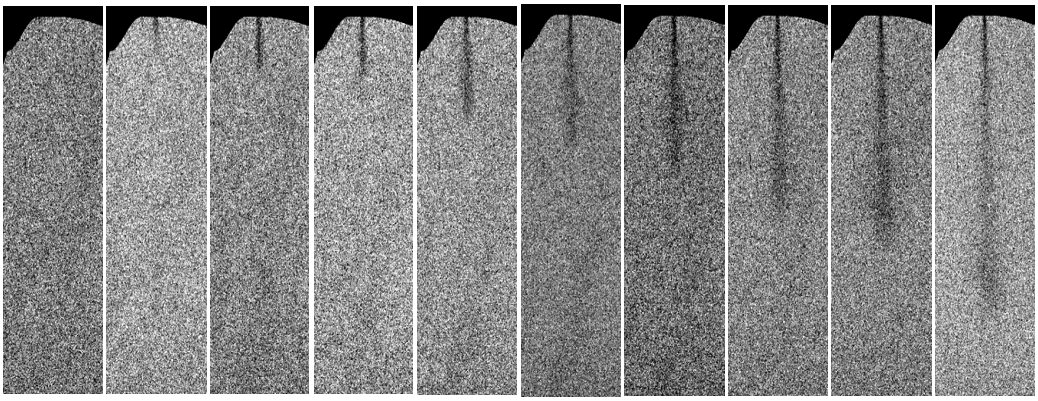

**Figure 6.** Expansion of dodecane/cerium spray through ks1.5, 6 hole, 110 µm in diameter orifices, production nozzle. Rail pressure 800 bars, injection 500 µs, chamber pressure 1 bar. Each radiograph is averaged over 1000 injection events. The time increment is of 10 µs from start of injection on the left to the righter picture 90 µs later for which the jet expands over 14 mm.

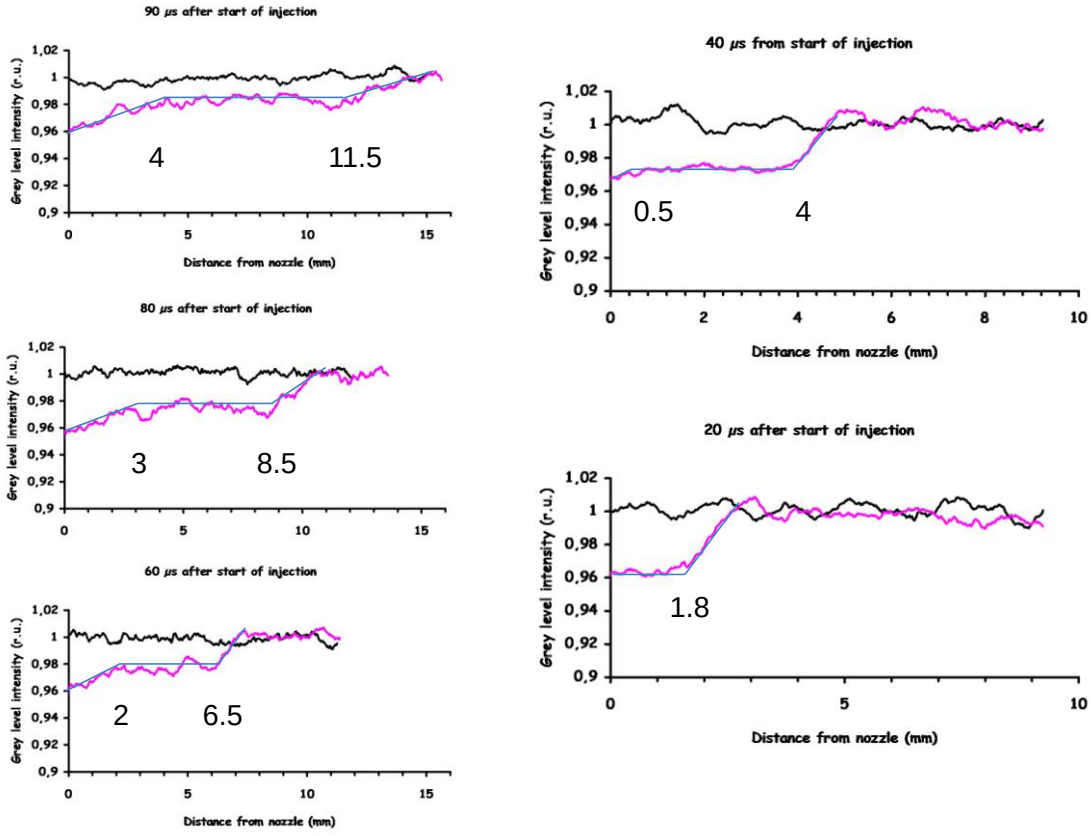


**Figure 7.** Longitudinal profiles from radiographs of Fig.6. The dark, respectively light traces on each graph corresponds to the out respectively on, jet axis positions. The lines are proposed for clarity of discussion, the numbers indicates transition positions between the two or three phases of the jet longitudinal profiles (see text)

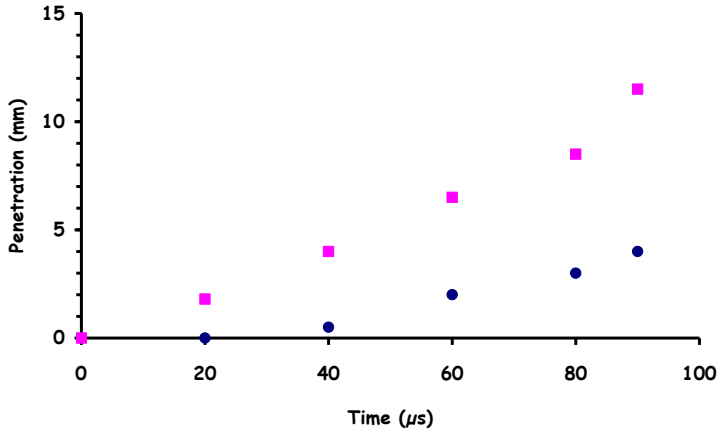


**Figure 8.** Dark dots, penetration of the "dense spray component". Light squares, penetration of the spray leading edge. Data corresponds to the longitudinal profiles of Fig. 7. traces are just data fits for clarity

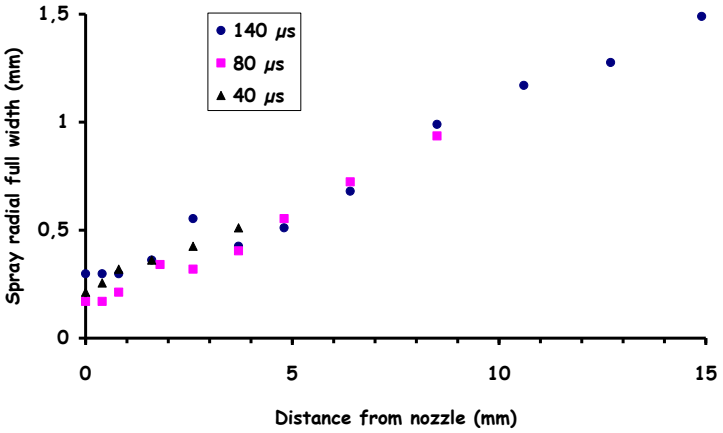


**Figure 9.** Evolution of the spray radial width versus downstream position for the three labelled delays. Data are extracted from radiographies in Fig.6. The first three downstream positions are longitudinally averaged over 0.4 mm, larger distances over 1.1 mm

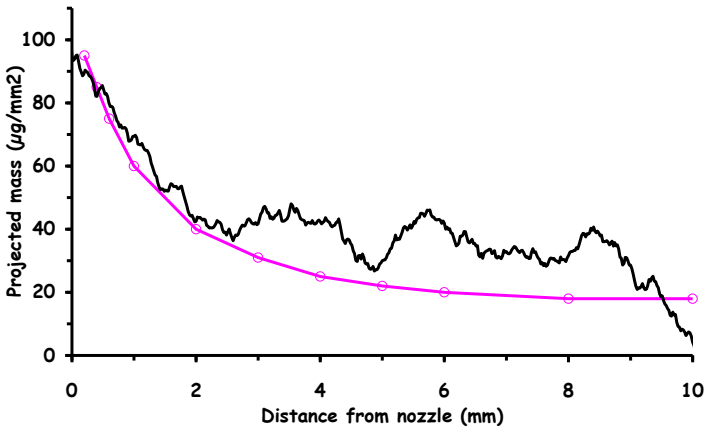


**Figure 10.** Dark trace: projected mass density versus downstream position. Data from Fig. 7, 80 µs instant, and accounting for the jet cone expansion documented in Fig. 9. Light open dots and corresponding light fitting trace are reproduced from [19], Figure 5a, 5- hole, gas density of 1.4 kg/m$^3$

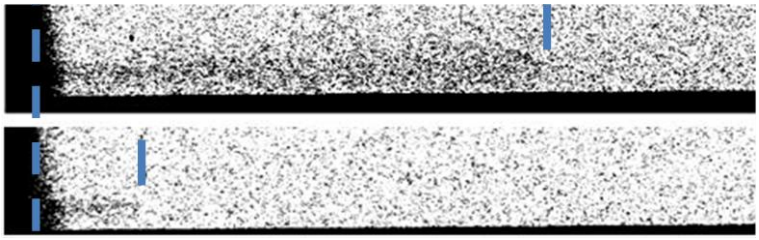

**Figure 11.** Expansion of dodecane/cerium spray through ks1.5, 6 hole, 110 µm in diameter orifices, production nozzle. Rail pressure 800 bars, injection 500 µs, chamber pressure 25 bars. Each radiograph is averaged over 1000 injection events. The delay with respect to start of the injection is of 20 µs for botton radiograph and 70 µs for upper radiograph. The dashed mark stands for the nozzle outlet position, full marks roughly indicate the spray leading edge for each delay